

## Yields and composition changes in low-energy sputtering of binary alloys: Experiments and computer simulations

H. Gnaser and H. Oechsner

*Fachbereich Physik, Universität Kaiserslautern, W-6750 Kaiserslautern, Germany*

(Received 4 September 1992; revised manuscript received 4 February 1993)

Emission-angle-integrated yields of neutral atoms and molecules ejected from binary alloys ( $\text{Cu}_{0.63}\text{Zn}_{0.37}$ ,  $\text{Ni}_{0.8}\text{W}_{0.2}$ ,  $\text{Cu}_{0.28}\text{W}_{0.72}$ ) due to  $\text{Ar}^+$  and  $\text{Xe}^+$  impact in the energy range from 30 to 1000 eV were determined by means of sputtered-neutral mass spectrometry using a hemispherical specimen arrangement. The yields of small homo- and heteronuclear molecules exhibit a dependence on the respective atom yields, which is characteristic of a statistical formation mechanism and is valid down to very low energies ( $\sim 100$  eV). Compositional changes of the near-surface concentration and the fluence-dependent evolution of partial atomic yields were investigated for  $\text{Ni}_{0.8}\text{W}_{0.2}$  by means of the binary-collision computer code T-DYN. The same projectiles and a similar energy range as in the experiments were used. The simulations produce a pronounced surface enrichment of W with steady-state concentrations ranging from  $>0.9$  at 50-eV impact energy to  $\sim 0.4$  for 2000 eV, while the yields of Ni and W exhibit a decrease and increase, respectively, with bombarding fluence. For both atomic species, the steady-state yields obtained from the simulations show a good agreement with the respective experimental data with the possible exception of very low energies. Also, transients in the yield evolution towards steady-state conditions have been monitored for selected impact energies and agree very well with corresponding simulation runs.

### I. INTRODUCTION

In recent years, studies of the sputtering of multicomponent specimens<sup>1-3</sup> strongly increased in number due to the advances of thin-film deposition processes by means of sputtering techniques. An important example is the production of homogeneous thin films from a single target (e.g., high-temperature superconductors). While for these kind of applications low bombarding energies are ubiquitous,<sup>4</sup> this energy regime is interesting also from a more basic point of view. At higher energies (say, above some keV) sputtering for conducting samples is governed by the development of a collision cascade of moving target atoms; this process is well described by analytical theory<sup>5,6</sup> and its predictions with respect to relevant parameters (e.g., total yields, energy distributions of sputtered species) generally show a good agreement with experimental data. At low and near-threshold impact energies, on the other hand, single-collision events increase in importance and may even dominate the sputter ejection from the surface. It is that regime which appears less accessible to a theoretical description, but for which also variations in various yield parameters (angular distribution,<sup>7</sup> changes of stoichiometry for multicomponent systems<sup>8</sup>) are most drastic.<sup>9</sup> We note that computer simulations<sup>10,11</sup> have considerably increased here the understanding of the operating mechanisms. Also, with respect to the composition of the sputtered flux (atoms versus molecules) this low-energy range appears of considerable importance; this is due to the fact that with decreasing impact energy the ejection process is becoming a very rare event and yield fluctuations<sup>12</sup> will be large. These might show up, for example, in the yield of sputtered molecules.

In two previous studies<sup>13,14</sup> we have investigated the sputtering of pure Ni and Cu in the low-energy regime (30–1000 eV) in order to elucidate further the mechanism of small-molecule formation. The present work is an extension of that approach towards binary alloys. Apart from an experimental determination of the yields of neutral atoms and molecules by means of a mass-spectrometric technique, computer simulations using the binary-collision approximation were carried out to study ion-impact-induced stoichiometric changes of the specimen's near-surface concentration. Furthermore, a comparison of pertinent experimental and simulation data is conducted.

### II. EXPERIMENTAL

The experiments were carried out in a sputtered-neutral mass spectrometer (Leybold INA-3) described in detail elsewhere.<sup>15</sup> The electron component (density  $\sim 10^{10}$   $\text{cm}^{-3}$ ) of a low-pressure ( $\sim 1.5 \times 10^{-3}$  Torr) rf plasma sustained by electron-cyclotron wave resonance<sup>16</sup> is employed for postionizing sputtered-neutral species. Ions are extracted from this plasma and accelerated onto the target, which is biased negatively to effect sputtering. From Langmuir-probe measurements the plasma potential (about +30 V) was determined; the ion's impact energy is higher by this amount than the actual target potential. Because of the moderately low temperature of the plasma electrons ( $\sim 6$  eV), production of and bombardment by doubly charged plasma ions is negligible. Current densities amount to about 1 mA/cm<sup>2</sup>. Leaving the plasma, postionized neutral species are guided into the quadrupole mass filter by means of two sets of electrostatic lenses and a broad-bandpass energy analyzer.

Hemispherical samples with a radius of  $\sim 2.5$  mm were manufactured from high-purity, polycrystalline alloys of  $\text{Cu}_{0.63}\text{Zn}_{0.37}$ ,  $\text{Cu}_{0.28}\text{W}_{0.72}$ , and  $\text{Ni}_{0.8}\text{W}_{0.2}$ . They were mounted on the sample holder of the instrument in a way<sup>13</sup> that their convex surface faces the entrance aperture of the mass spectrometer, while the plane rear side was about 6 mm from the actual specimen holder. The distance from the sample to the spectrometer entrance, i.e., the flight length through the plasma amounted to  $\sim 25$  mm. Contrary to the ordinary operation of the instrument, the samples employed in this work were completely immersed into the plasma to achieve homogeneous, normal-incidence ion bombardment, the remaining parts of the specimen holder were shielded from (high-energy) particle impact by means of insulating ceramics. At the pressure used in this study the mean-free-path length amounts to about 60 mm; thus, scattering of sputtered species on their way through the plasma should be of minor importance. In addition, any such influence on the sputtered flux should not depend on the main parameters varied in the experiments, namely the primary bombarding energy and the sample composition.

### III. COMPUTER SIMULATION

The preferential sputtering and the development of an altered near-surface layer have been simulated for the NiW alloy using the PC-version [T-DYN 4.0 (Ref. 17)] of the binary-collision Monte Carlo code TRIDYN.<sup>18,19</sup> This program is based on the TRIM code<sup>20,21</sup> and allows a dynamic rearrangement of the local composition of the target; thus, effects in high-fluence ion implantation, ion mixing, and preferential sputtering caused by atomic collision processes can be studied. The basic features of TRIDYN and several applications<sup>22,23</sup> have been described in the literature. In brief, elastic binary collisions between incident projectiles and cascade atoms are calculated employing the Kr-C interaction potential.<sup>24,25</sup> A planar surface potential is used with different surface-binding energies  $E_s$  for the two constituents, but independent of the momentary surface composition. The pure elements' cohesive energies<sup>26</sup> were chosen, i.e.,  $E_s(\text{Ni})=4.5$  eV and  $E_s(\text{W})=8.7$  eV. As another input parameter, the code requires bulk binding energies  $E_b$ ; by this amount the energy of a recoil atom hit in a collision is reduced. While previous applications of TRIDYN frequently used  $E_b=0$ , the influence of the magnitude of  $E_b$  on various calculated data was investigated here (see below). Comparing pure-element sputtering yields with data obtained by the static TRIM code<sup>21</sup> led to a choice of  $E_b=1$  eV for both Ni and W. The trajectory of an atom was followed until its energy falls below a cutoff value  $E_c$ , and  $E_c=3$  eV was used here.

The simulations were run for Ar and Xe as projectiles and impact energies from 40 eV to 2 keV. Incident numbers were chosen to reach steady-state conditions with respect to partial sputtering yields and near-surface composition. "Pseudo"-fluences thus obtained ranged from  $10^{16}$  to about  $10^{19}$   $\text{cm}^{-2}$ ; actual runtimes varied from a few hours to about 25 h on a 386-based personal computer.

## IV. RESULTS AND DISCUSSION

### A. Yields of atoms and molecules

In previous studies<sup>13,14</sup> we have investigated the low-energy (near-threshold) sputtering from pure nickel and copper specimens. Concerning the emission of atoms and small molecules (dimers and trimers) two essential features could be recognized:

(i) Down to very low-impact energies ( $< 100$  eV) the yields of small  $n$ -atom clusters  $A_n$  were found<sup>14</sup> to scale with the  $n$ th power of the average number of atoms  $A$  sputtered per collision cascade  $Y(A)$ ,

$$Y(A_n) \propto [Y(A)]^n. \quad (1)$$

Such a yield dependence is indicative of a formation mechanism<sup>27-29</sup> proceeding via a combinative association of atoms ejected individually (albeit closely correlated with respect to their momenta) from the same collision cascade.

(ii) At low bombarding energies a distinct influence of the variation of the sputtered particles angular distribution on the yields of atoms and molecules was noticed.<sup>13,14</sup> This effect was demonstrated by a comparison of results obtained employing hemispherical samples (thereby integrating over all emission directions) with those from planar samples which correspond to a narrow acceptance angle along the surface normal. In fact, using the former arrangement, the agreement of the data with Eq. (1) was much improved as compared to the angle-selected experiments.

In this work those studies were extended to binary alloys to verify<sup>30</sup> the validity of Eq. (1) for heteronuclear molecules and to investigate the effects of preferential sputtering on partial sputtering yields. Furthermore,  $\text{Xe}^+$  was used as a projectile in addition to  $\text{Ar}^+$ .

Figure 1 shows for hemispherical samples of  $\text{Cu}_{0.63}\text{Zn}_{0.37}$  and  $\text{Cu}_{0.28}\text{W}_{0.72}$  the intensities (normalized to the bombarding current) of various sputtered neutral species as a function of ion-impact energy. All data were recorded at steady-state conditions, i.e., for a near-surface composition which may deviate (pronouncedly) from the bulk values. Apart from the atomic species, also the signals of molecules could be measured to very low energies ( $< 100$  eV). It is noted, however, that the plotted data do not necessarily represent the actual sputtered flux; this is due to the unknown ionization and dissociation cross sections of the different species. On the other hand, these are not expected to depend on the impact energy; therefore, the given yield-vs-energy curves for any single species reflect the dependence of the partial sputtering yields on the bombarding energy. Data similar to those depicted in Fig. 1 have been obtained for the NiW alloy.

Figure 2 shows for the three alloys investigated the ratio of atomic yields as a function of the impact energy. Again, the data refer to steady-state sputtering as indicated by constant ion signals. While for the CuZn alloy the ratio  $Y(\text{Zn})/Y(\text{Cu})$  is essentially constant (less than 20% variation between 40 eV and 1 keV) and  $Y(\text{Sn})/Y(\text{Cu})$  falls within a factor of 2 (Sn is a 0.1 at. % impurity in this

specimen), for both CuW and NiW the yield ratios exhibit drastic variations with bombarding energy. They are most pronounced for energies below  $\sim 200$  eV. Ideally, the use of hemispherical samples, should, as discussed in Ref. 13, compensate for any variation of the sputtered neutrals' angular emission distribution. The actual experimental arrangement (e.g., the finite distance between the sample and the spectrometer entrance aperture) might entail some limitations to that model assumption. The possible influence of such an effect should be most drastic at low irradiation energies: In this regime angular distributions of sputtered atoms exhibit considerable variations<sup>7</sup> and can be different for the different species of a multicomponent sample, in particular if concentration gradients exist within the sputtered particles escape depth.<sup>1,6</sup> Because of the large mismatch in mass and binding energy between W on the one hand and Cu or Ni on the other (causing, probably, distinct differences in the emission distributions) such differences in angular distributions are expected for the NiW and CuW specimens, but are probably absent for CuZn and, together with the aforementioned incomplete compensation, they may

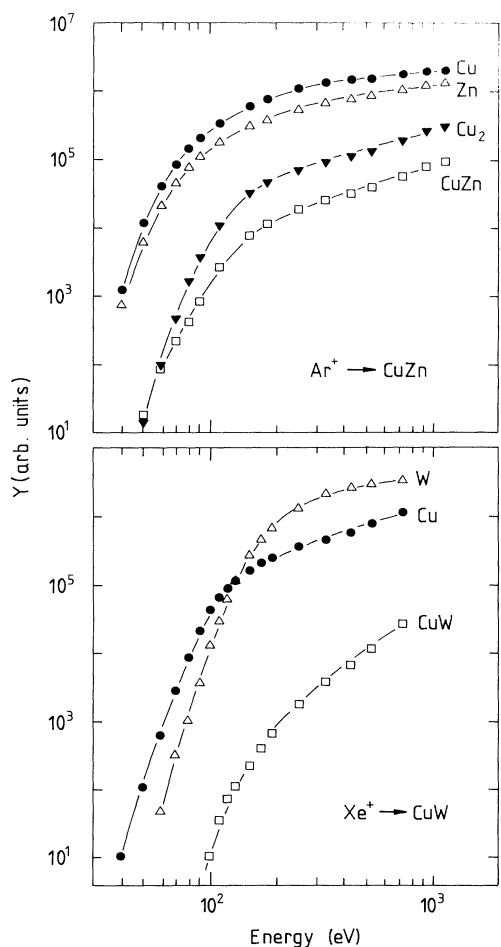


FIG. 1. Steady-state yields of atomic and molecular species sputtered from  $\text{Cu}_{0.63}\text{Zn}_{0.37}$  and  $\text{Cu}_{0.28}\text{W}_{0.72}$  as a function of the impact energy. Solid lines are drawn to guide the eye.

cause the variation of the yield ratios at low-impact energies.

Due to the statistical nature of the formation mechanism governing the emission of small molecules,<sup>28-30</sup> also heteronuclear species are expected to obey a correlation similar to Eq. (1). Therefore, the yield of a molecule  $AB$

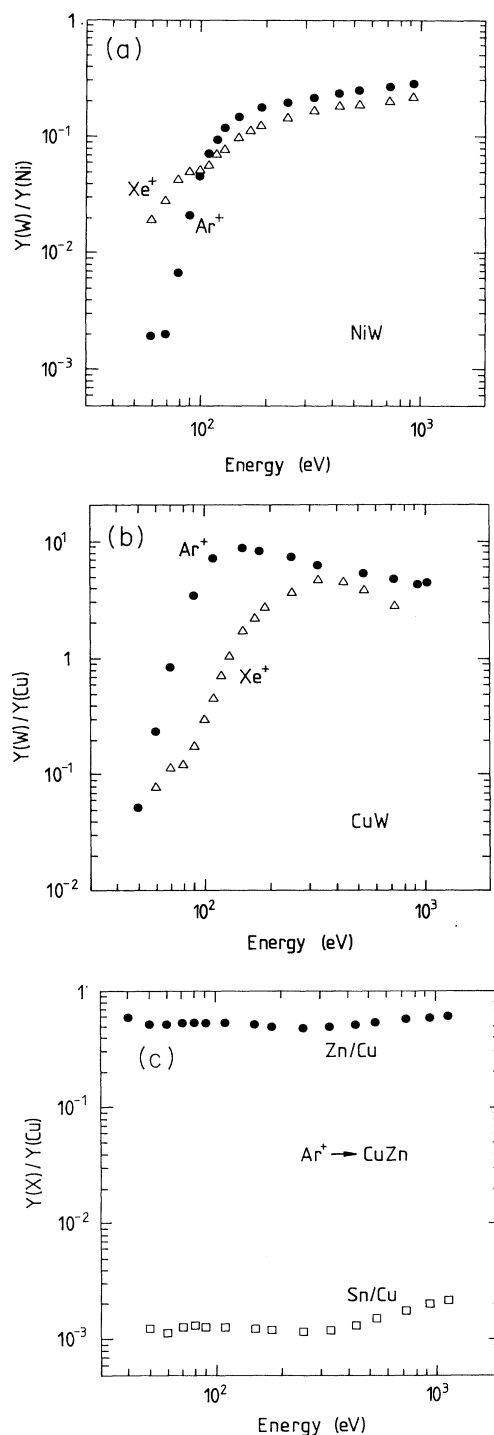


FIG. 2. Yield ratio of atomic species vs bombarding energy for the projectiles and samples indicated.

should be proportional to the product of the partial yields  $Y(A)$  and  $Y(B)$ :

$$Y(AB) \propto Y(A)Y(B). \quad (2)$$

Figure 3(a) depicts such a dependence for  $\text{Ar}^+$  bombardment of the NiW alloy. A very good linear correlation according Eq. (2) is found featuring a correlation coefficient of 0.998. A log-log representation of these data reveals a linear dependence over more than two orders of magnitude in yield variation. Figure 3(b) shows similar data of  $Y(\text{CuZn})$  yields; again a linear dependence in agreement with Eq. (2) is found.

Apart from the heteronuclear molecules also the yields of  $\text{Ni}_2$  and  $\text{Ni}_3$  sputtered from NiW (Fig. 4) exhibit dependencies in accordance with Eq. (1), thus confirming the validity of our observation on pure Ni (Ref. 14), and extending it to the Ni-W binary system. This appears to

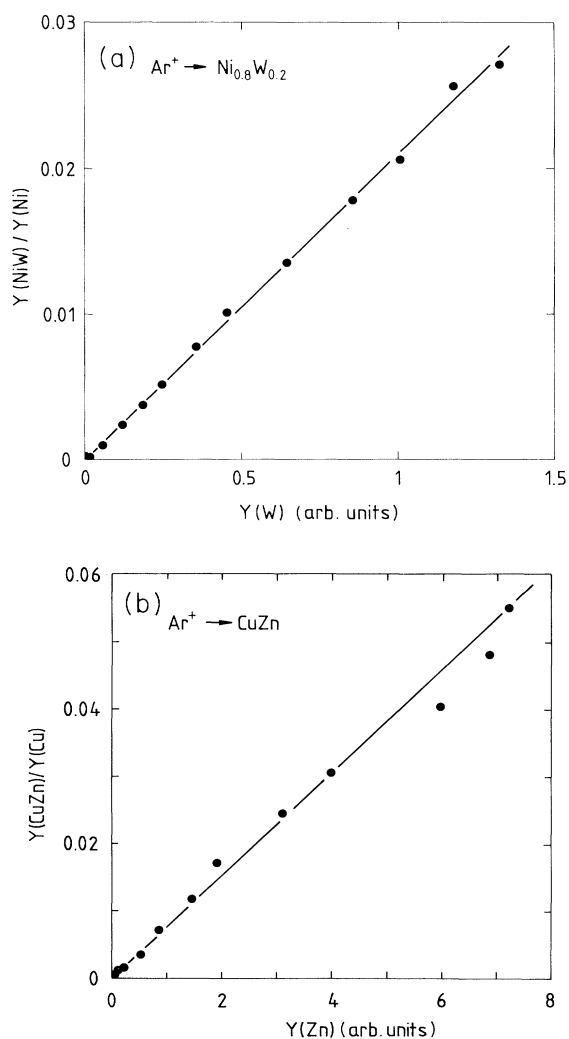


FIG. 3. The relative yield of sputtered NiW molecules,  $Y(\text{NiW})/Y(\text{Ni})$  as a function of the atomic yield  $Y(\text{W})$  (a) and of sputtered CuZn molecules,  $Y(\text{CuZn})/Y(\text{Cu})$  as a function of atomic yield  $Y(\text{Zn})$  (b). The data refer to steady-state conditions. The solid lines are linear least-square fits.

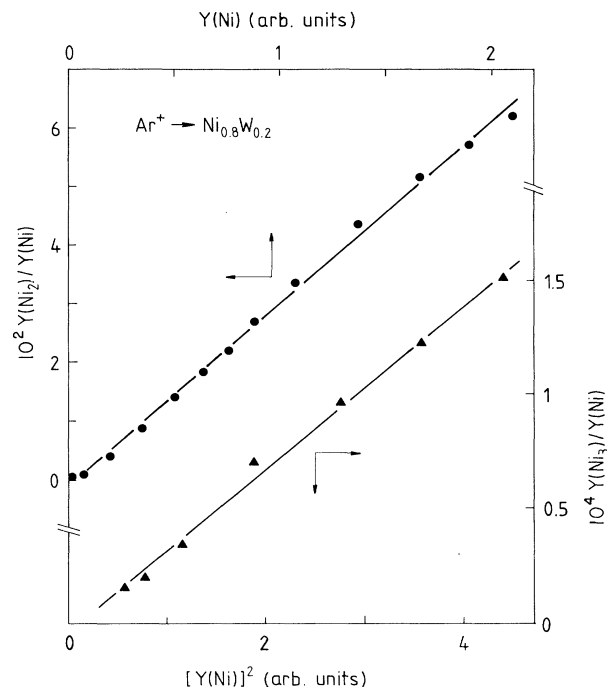


FIG. 4. Relative dimer  $Y(\text{Ni}_2)/Y(\text{Ni})$  and trimer  $Y(\text{Ni}_3)/Y(\text{Ni})$  yield ratios vs the atomic yields and the atomic yield squared  $[Y(\text{Ni})]^2$ , respectively. Solid lines are linear least-square fits.

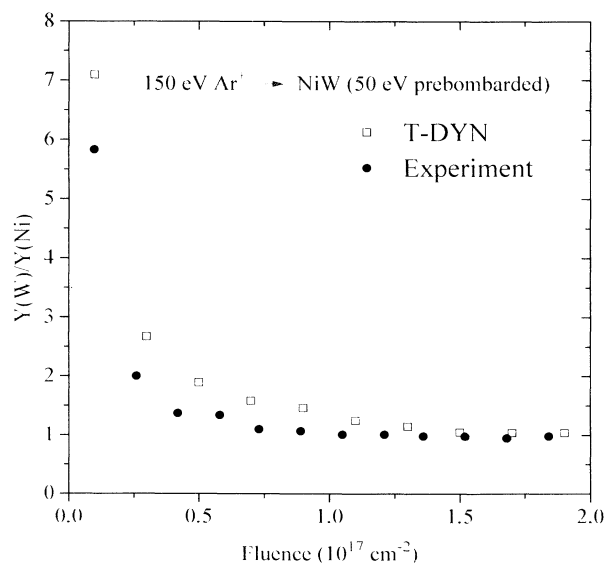


FIG. 5. Evolution of the yield ratio  $Y(\text{W})/Y(\text{Ni})$  (normalized to the stationary value) vs fluence for 150-eV  $\text{Ar}^+$  bombardment of a NiW specimen which has been subjected before to 50-eV  $\text{Ar}^+$  impact until steady-state conditions were reached. Experimental data are compared with the outcome of a T-DYN simulation run.

TABLE I. Simulation results of steady-state sputtering yields,  $Y(\text{Ni})$  and  $Y(\text{W})$ , W surface concentration,  $c^s(\text{W})$ , and the fluence necessary to reach equilibrium,  $\phi^\infty$ , for different sets of bulk energies  $E_b(\text{Ni})$  and  $E_b(\text{W})$ . The calculations refer to Ar-impact energies of 75 and 300 eV and surface-binding energies  $E_s(\text{Ni})=4.5$  eV and  $E_s(\text{W})=8.7$  eV.

|        | $E_b(\text{Ni})$ | $E_b(\text{W})$ | $Y(\text{Ni})$ | $Y(\text{W})$ | $c^s(\text{W})$ | $\phi^\infty$            |
|--------|------------------|-----------------|----------------|---------------|-----------------|--------------------------|
|        | (eV)             |                 | (atoms/ion)    |               |                 | ( $10^{17}$ cm $^{-2}$ ) |
| 75 eV  | 0.1              | 0.1             | 0.055          | 0.013         | 0.85            | 7                        |
|        | 1.0              | 1.0             | 0.043          | 0.0094        | 0.87            | 7                        |
|        | 1.0              | 4.0             | 0.017          | 0.003         | 0.93            | 9                        |
|        | 4.5              | 8.7             | 0.0092         | 0             | 0.94            | 9                        |
| 300 eV | 0.1              | 0.1             | 0.56           | 0.13          | 0.55            | 0.8                      |
|        | 1.0              | 1.0             | 0.49           | 0.12          | 0.55            | 1.1                      |
|        | 4.5              | 8.7             | 0.28           | 0.067         | 0.56            | 1.2                      |

be an indication that the atoms forming, e.g.,  $\text{Ni}_2$  do not necessarily originate from contiguous positions on the sample surface. This is because at bombarding energies of less than 100 eV, where Eq. (1) still is valid for  $\text{Ni}_2$ , the stationary surface concentration is less than 10% (see below); therefore, the average distance between any two Ni atoms on the surface is fairly large. There exists, however, the possibility that even at a low average concentration of one of the components these atoms may agglomerate into islands of pure material; such a situation should occur if the different atoms of an alloy have a positive heat of mixing.<sup>2</sup>

### B. Transients in yields and surface composition

Experimental results presented so far referred to steady-state conditions for which a stationary near-surface composition is established and the sputtered flux corresponds to the bulk values. The transients to reach this equilibrium are difficult to observe in our experimental arrangement, largely because of the high-ion-flux densities ( $\sim 6 \times 10^{15}$  ions/cm $^2$  sec) and a correspondingly limited number of data points. Nevertheless, for some selected energies experimental runs were carried out and compared with the respective outcome from T-DYN simulations. Figure 5 depicts the temporal evolution of the yields of Ni and W sputtered from the NiW alloy due to 150-eV  $\text{Ar}^+$  impact. Before starting this run, the Ni-W specimen has been prebombarded by 50-eV  $\text{Ar}^+$  ions to a fluence sufficient for establishing equilibrium conditions. Figure 5 therefore exemplifies the transient from the 50-

eV steady-state yield to that at 150 eV. Figure 5 presents in addition data obtained by computer simulations employing conditions identical to the experimental ones, i.e., the final compositional profile of a 50-eV run was used as starting point for a 150-eV bombarding run. In passing it is noted that at 50-eV  $\text{Ar}^+$  energy the stationary surface concentration of W is about 0.95, while it falls to roughly 0.65 for 150-eV  $\text{Ar}^+$  impact (see also, Sec. IV C).

The fairly good agreement between the experimental and computer runs also indicates that the input parameters (binding energies) chosen for the latter are reasonable: In fact, additional runs using other values compare less favorably with the experiment (in particular, the fluence to reach the 150-eV steady-state condition is very sensitive towards the values of the bulk binding energies).

### C. Computer simulations of preferential sputtering

The computer code T-DYN (Ref. 17) was used to determine partial yields and preferential sputtering for a binary  $\text{Ni}_{0.8}\text{W}_{0.2}$  alloy. As noted in Sec. III, the outcome of the simulations exhibits a dependence on the binding energy values used as input parameters. To elucidate these influences and to assess their importance, several simulation runs were carried out using various sets of values for the surface and bulk binding energies of Ni and W; it appears to be especially the latter parameter for which a reasonable value in computer simulation of the present type employing binary-collision approximations is difficult to establish. Table I compiles for 75- and 300-

TABLE II. Simulation results of steady-state sputtering yields, W surface concentration  $c^s(\text{W})$ , and the equilibrium fluence  $\phi^\infty$  for different sets of surface-binding energies  $E_s(\text{Ni})$  and  $E_s(\text{W})$ . The calculations refer to Ar-impact energies of 75 and 300 eV and bulk binding energies  $E_b(\text{Ni})=E_b(\text{W})=1$  eV.

|        | $E_s(\text{Ni})$ | $E_s(\text{W})$ | $Y(\text{Ni})$ | $Y(\text{W})$ | $c^s(\text{W})$ | $\phi^\infty$            |
|--------|------------------|-----------------|----------------|---------------|-----------------|--------------------------|
|        | (eV)             |                 | (atoms/ion)    |               |                 | ( $10^{17}$ cm $^{-2}$ ) |
| 75 eV  | 4.5              | 8.7             | 0.043          | 0.0094        | 0.87            | 6.5                      |
|        | 4.5              | 6.7             | 0.075          | 0.019         | 0.75            | 6.0                      |
|        | 4.5              | 4.5             | 0.114          | 0.029         | 0.5             | 4.0                      |
| 300 eV | 4.5              | 8.7             | 0.49           | 0.125         | 0.55            | 1.1                      |
|        | 4.5              | 6.7             | 0.55           | 0.134         | 0.45            | 1.0                      |
|        | 4.5              | 4.5             | 0.63           | 0.16          | 0.32            | 0.9                      |

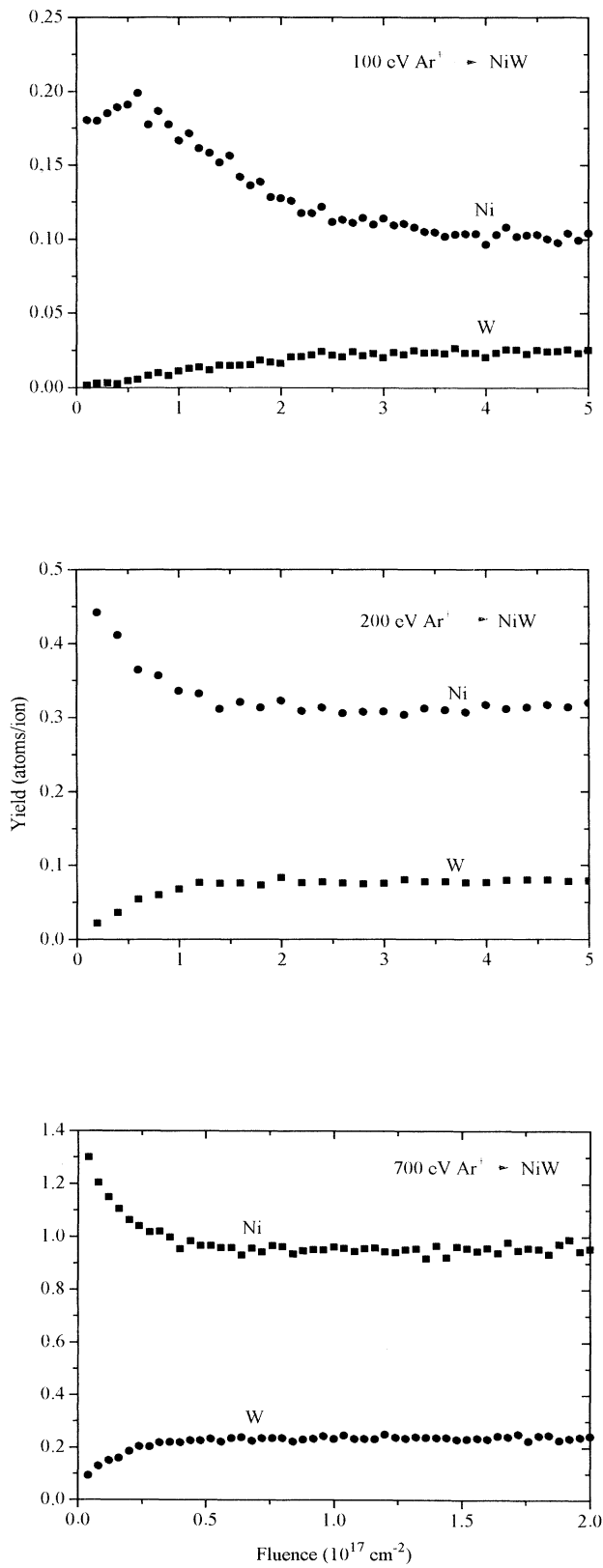


FIG. 6. For different Ar bombarding energies, the partial sputtering yields of Ni and W as derived from the simulations are plotted vs the fluence.

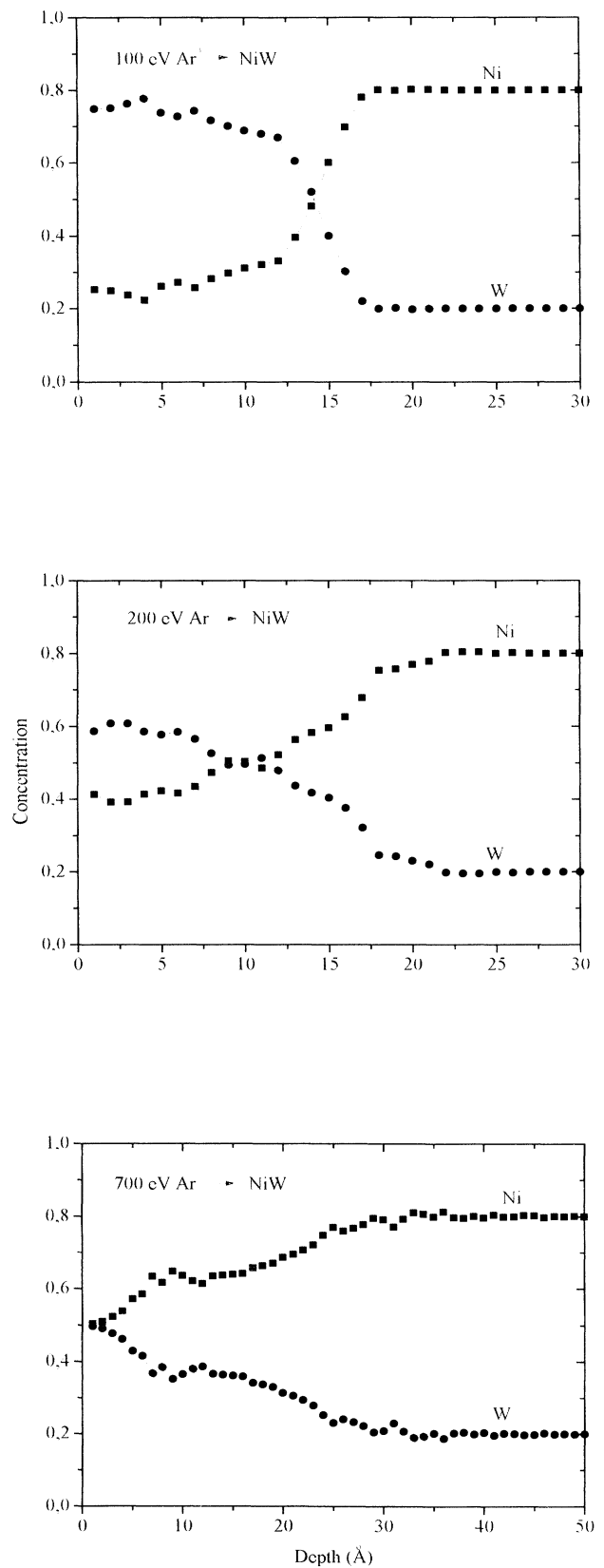


FIG. 7. T-DYN composition profiles of Ni and W for steady-state conditions and different bombardment energies.

eV Ar<sup>+</sup> impact the output data from the various runs. Specifically, the stationary surface concentration of W,  $c^s(\text{W})$ , the partial steady-state yields of Ni and W,  $Y(\text{Ni})$  and  $Y(\text{W})$ , respectively, and the fluence necessary to establish equilibrium conditions  $\phi^\infty$ , are listed for different sets of bulk binding energies  $E_b(\text{Ni})$  and  $E_b(\text{W})$ . While the value of  $c^s(\text{W})$  and  $\phi^\infty$  exhibit comparatively little dependence on  $E_b$ , the influence is dramatic for the yield values; in particular,  $Y(\text{W})$  varies between 0 and about 0.01 for the lowest and the highest values of  $E_b$  for 75-eV Ar. At 300-eV bombardment there is essentially no dependence of  $c^s(\text{W})$  and  $\phi^\infty$  on  $E_b$  and the variations of  $Y$  fall within a factor of 2. Also, in that range the thickness of the altered layer decreases from about 18 to 12 Å; since these values exceed the sputtered atoms escape depths, that variation is probably of little importance in the present context.

Table II lists, again for 75- and 300-eV Ar bombardment, the same output data for three sets of surface-binding energies. The first one employs the cohesive energies of the pure elements. Kelly<sup>31,32</sup> has argued that such a choice is incorrect "since the binding in an alloy is governed in all cases by the statistics of site occupancy."<sup>32</sup> For a Ni<sub>0.5</sub>W<sub>0.5</sub> alloy he derives a surface-binding energy ratio  $E_s(\text{W})/E_s(\text{Ni})=1.4$ . The second set of data given in Table II [ $E_s(\text{Ni})=4.5$  eV,  $E_s(\text{W})=6.7$  eV] closely corresponds to this proposal. This choice produces, for the low-ion energy, a twofold increase of the partial sputtering yields and a 15% reduction of the W surface concentration. For the 300-eV case the yield enhancement (roughly 10%) is moderate compared to the first data set. Finally, simulation runs were performed using identical surface-binding energies for both constituents. Again, the variations are seen to be most pronounced for the low-energy case. As in most previous simulations applying the binary-collision approximation<sup>18-23</sup> the

cohesive energies of the pure substances were used as surface-binding energies [i.e.,  $E_s(\text{Ni})=4.5$  eV,  $E_s(\text{W})=8.7$  eV].

For bulk binding energies values of  $E_b(\text{Ni})=E_b(\text{W})=1$  eV were chosen, mostly for two reasons: First, T-DYN runs simulating a pure Ni sample and using  $E_b=1$  eV resulted in a sputtering yield ( $Y \approx 0.05$  atoms/ion for 75-eV Ar<sup>+</sup>) identical with that reported by the (static) TRIM code.<sup>21</sup> Second, energies for vacancy formation are on the order of 0.5–1 eV for many fcc metals and slightly higher for a bcc crystalline structure.<sup>33</sup>

In the following some exemplary output from the simulations will be presented, succeeded by a comprehensive compilation of the relevant data obtained for both projectiles and the complete energy range covered. Figure 6 depicts the evolution of the partial sputtering yields  $Y(\text{Ni})$  and  $Y(\text{W})$  as a function of bombarding fluence for different Ar<sup>+</sup> ion energies. With increasing fluence the partial yield of W increases, while  $Y(\text{Ni})$  decreases; the latter, however, passes through a maximum for  $E < 100$  eV. Apart from this feature, the generally observed yield variations reflect the gradual enrichment of the near-surface region in tungsten and the corresponding depletion in nickel. Upon completion of this transient caused by the preferential ejection and/or relocation of Ni, the composition of the sputtered flux is equivalent to that of the bulk stoichiometry. The transients are more pronounced at low-impact energies due to the stronger W-surface enrichment.

This can be seen in Fig. 7, which shows the stationary near-surface composition profiles of Ni and W for the same impact energies as shown in Fig. 6. While  $c^s(\text{W})$  approaches 100% near the surface for  $E=50$  eV,  $c^s(\text{W}) \sim 0.5$  only at 500 eV. As expected, however, the altered layer extends deeper into the solid, but even at the lowest energies applied here it by far exceeds the average

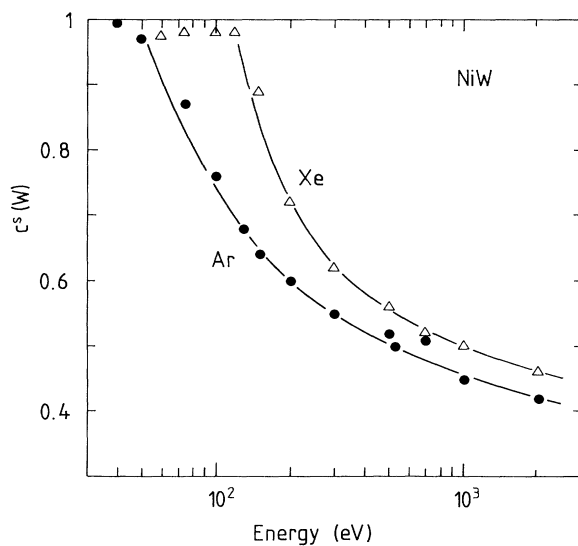


FIG. 8. Stationary surface concentration of W,  $c^s(\text{W})$  as derived from the simulations as a function of impact energy for Ar and Xe projectiles. Solid lines are drawn to guide the eye.

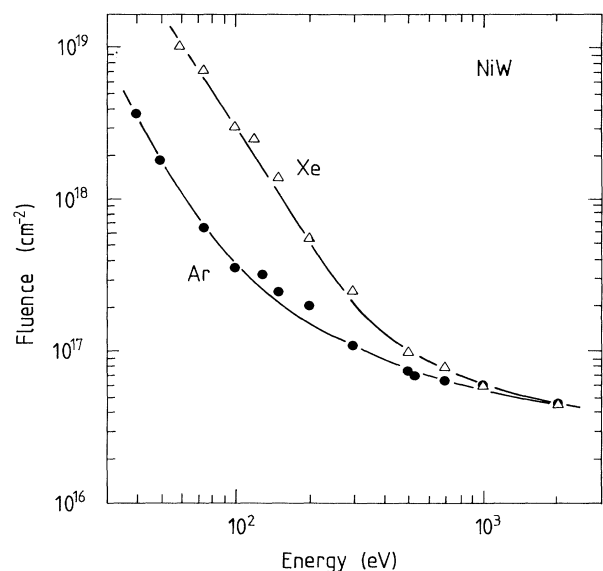


FIG. 9. Fluence at which steady-state conditions are reached in the simulations vs bombarding energy of Ar and Xe.

escape depth of the sputtered atoms. Although we have not recorded the latter quantity, previous data<sup>34</sup> indicate that it probably also increases (slightly) with impact energy.

For both projectile species used in the simulations, Fig. 8 compiles the steady-state surface concentration  $c^s(W)$  as a function of bombarding energy; Fig. 9 plots the fluence  $\phi^\infty$  necessary to reach that stationary condition. Both quantities are seen to increase sharply with decreasing impact energy; that rise is more pronounced for  $Xe^+$  than for  $Ar^+$ . Noteworthy is the fact that  $c^s(W)$  for the highest values of  $E$  (2 keV) still amounts to about twice the bulk concentration; also an extrapolation to higher energies indicates only a very gradual decrease.

For the linear collision cascade regime Andersen and Sigmund<sup>35</sup> derived an expression for the preferential sputtering based on the use of power cross sections as approximations to the screened Coulomb interaction potential. According to that approach<sup>1,35,36</sup> the ratio of the stationary surface concentrations in a binary system is given (here for NiW) by

$$\frac{c^s(Ni)}{c^s(W)} = \frac{c^b(Ni)}{c^b(W)} \left[ \frac{E_s(Ni)}{E_s(W)} \right]^{1-2m} \left[ \frac{M_{Ni}}{M_W} \right]^{2m}, \quad (3)$$

where  $c^b$  is the bulk concentration,  $M$  the mass of the species, and  $m$  is the exponent of the power-law potential. For the interaction potential employed in the simulation  $m \sim 0.16$ .<sup>34</sup> With this value, Eq. (3) can be used to evaluate  $c^s(W)$  and  $c^s(W) = 0.36$  is found. While this is comparable to the high-energy data of the simulations, the theoretical approach<sup>35,36</sup> does not predict the pronounced

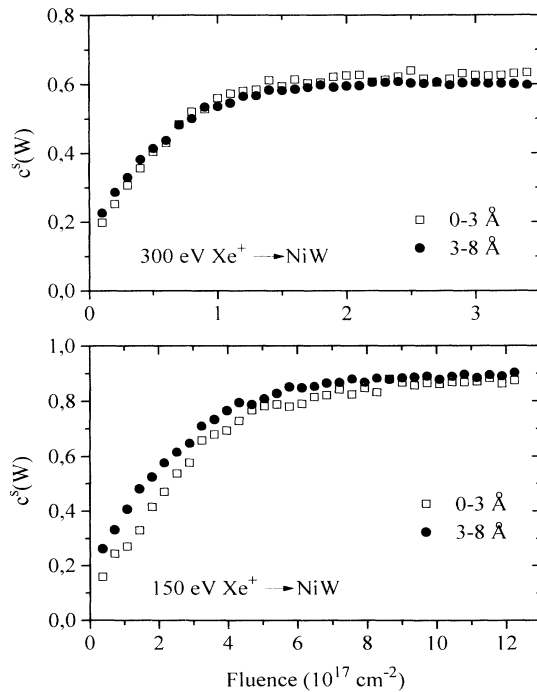


FIG. 10. W surface concentration  $c^s(W)$  as a function of fluence for different bombarding energies. Parameter is the integration depth (0–3 Å and 3–8 Å, respectively).

dependence on impact energy. As mentioned in Sec. I, however, it might not be valid for near-threshold energies.

On the other hand, the strong W surface enrichment is in qualitative agreement with previous experimental investigations<sup>37</sup> on a similar specimen using Auger electron spectroscopy. There, a value  $c^s(W) = 1$  for 70-eV  $Ar^+$  impact was reported with  $c^s(W)$  decreasing to  $\sim 0.8$  at 500 eV and 0.6 at 1000 eV. Contrary to the present simulations, this study<sup>37</sup> revealed compositional gradients in the topmost surface layers of the specimen. The reason for this difference is not clear presently. Computer simulations<sup>38</sup> of a sample ( $Ni_{0.8}Mo_{0.2}$ ) similar to the one used here also produced a pronounced surface enrichment of the heavier and/or more strongly bound component (Mo) at very low bombarding energies. At 50-eV  $Ar$  impact

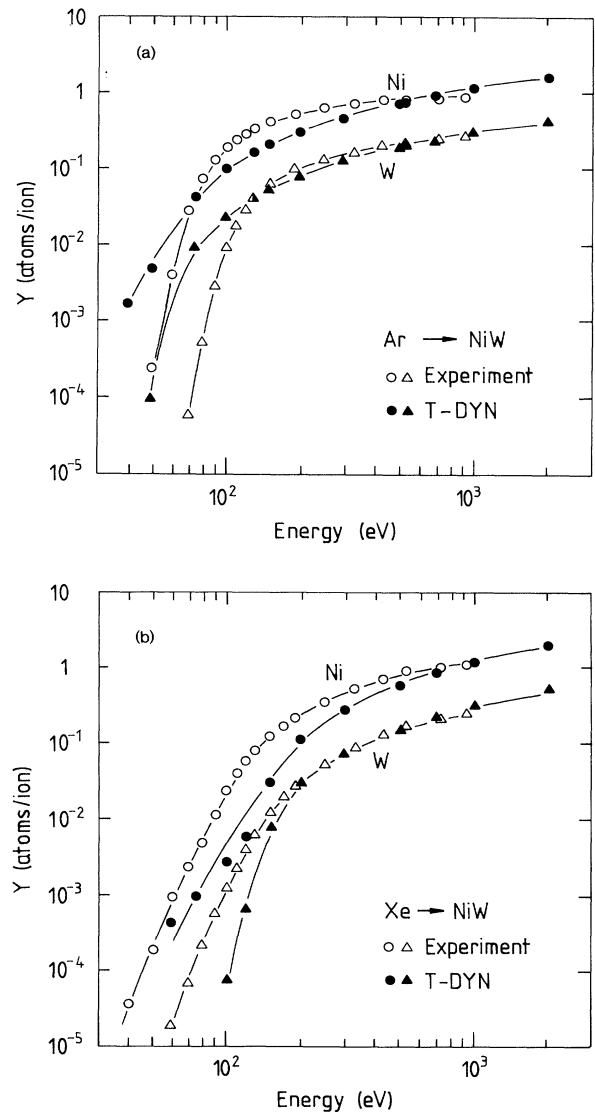


FIG. 11. Steady-state partial sputtering yields  $Y(Ni)$  and  $Y(W)$  as a function of impact energy for (a)  $Ar$  and (b)  $Xe$  projectiles. Compared are the results from the T-DYN simulations and the experiments. Solid lines are drawn as a guide to the eye.

$c^s(\text{Mo}) \sim 0.95$  is found, while for 1 keV Ar  $c^s(\text{Mo}) \sim 0.45$ .<sup>38</sup> Both values are in good agreement with the corresponding ones (0.97 and 0.44, respectively) obtained here (cf. Fig. 8).

The evolution of the W surface concentration as a function of fluence is shown in Fig. 10 for various bombarding parameters. In all cases an integration over two different depth ranges (0–3 Å and 3–8 Å, respectively) was performed. It can be seen that for low energies the W enrichment is initially more pronounced in the deeper-lying layer than at the surface. At medium and higher energies this situation tends to reverse. In fact, an inspection of the compositional profiles at various fluences indicates that for energies < 150 eV, appreciable composition changes take place in deeper layers, while the surface layer(s) stay essentially unchanged for fluences of less than about  $10^{17} \text{ cm}^{-2}$ . These concentration changes are most pronounced at a depth which roughly corresponds to the primary ions' project range but extend to a depth three times as large. Apparently, an efficient relocation mechanism (cascade and/or recoil mixing) is operative causing a depletion of Ni in that depth interval by transporting these atoms both closer to the surface and deeper into the bulk as compared to W atoms. The former process partly compensates the preferential ejection of Ni from the surface layer, thereby inducing the concentration gradients observed especially at low (and medium) fluences.

Figure 11 depicts the partial sputtering yields  $Y(\text{Ni})$  and  $Y(\text{W})$  for steady-state conditions as a function of energy again for both projectiles. Also given are the corresponding experimental data. Both data sets demonstrate that  $Y(\text{W})$  drops more pronouncedly than  $Y(\text{Ni})$  towards lower impact energies. In fact, the simulations indicate a threshold for the sputtering of W atoms by  $\text{Ar}^+$  on the order of 50 eV, while for Ni that value lies beyond the energy regime investigated (< 40 eV). For  $\text{Xe}^+$  impact the corresponding threshold values are found to be somewhat higher; a similar observation is derived from computer simulations of pure-element samples using TRIM.<sup>21</sup>

Comparison of the experimental results and the simulation data (see Fig. 11) for Ar bombardment reveals that the partial yields of Ni agree (within a factor of about 3) in the energy range from 70 eV to 1 keV; at lower energies, however, the experimental values of  $Y(\text{Ni})$  decrease

more strongly and at 40 eV the difference amounts to two orders of magnitude. A similar result is found for  $Y(\text{W})$ : Here the agreement for energies between 100 eV and 1 keV is even better (a factor of < 2), but again a strong divergence between experiment and simulation data is observed for lower energies. Qualitatively the same conclusions can be drawn from a comparison of the data due to Xe impact. A reason for the prominent discrepancies at near-threshold energies might be the breakdown of the validity of the binary-collision approximation inherent in the simulation code. From an inclusion of multiple interactions in atom collisions, as they will be typical in that energy regime, an increase of the sputtering yield can be expected, since additional ejection mechanisms might become operative.<sup>39,40</sup> The inclusion of such processes would therefore tend to increase the yield differences observed in the present work at low energies.

## V. CONCLUSIONS

The sputtering of binary alloys was investigated by experiments and computer simulations using Ar and Xe projectiles with impact energies ranging from 30 eV to 2 keV. The major observations were the following:

(i) Comparison of steady-state yields of Ni and W obtained by experiment and simulation show a reasonable agreement, with the latter exhibiting some dependence, in particular at low impact energies, on the energy parameters entering as input.

(ii) Yields of small molecules correlate with the respective atomic yields in a way indicative of their formation via the combinative association of individually but closely correlated sputtered atoms.

(iii) Compositional changes of the near-surface concentration as derived from the computer simulation data are characterized by a strong W enrichment; this species steady-state concentration amounts to about 0.9 at 50-eV bombarding energy and to  $\sim 0.4$  for 2 keV.

## ACKNOWLEDGMENT

We thank J. P. Biersack for providing a copy of the T-DYN computer code and for his helpful comments thereon.

<sup>1</sup>H. H. Andersen, in *Ion Implantation and Beam Processing*, edited by J. S. Williams and J. M. Poate (Academic, Sydney, 1984), p. 127.

<sup>2</sup>N. Q. Lam, in *Fundamentals of Beam-Solid Interactions and Transient Thermal Processing*, edited by M. J. Aziz, L. E. Rehn, and B. Stritzker, MRS Symposia Proceedings No. 100 (Materials Research Society, Pittsburgh, 1988), p. 29.

<sup>3</sup>R. Kelly, *Nucl. Instrum. Methods B* **39**, 43 (1989).

<sup>4</sup>J. J. Cuomo, S. M. Rossnagel, and H. R. Kaufman, *Handbook of Ion-Beam Processing Technology* (Noyes, Park Ridge, 1989).

<sup>5</sup>P. Sigmund, *Phys. Rev.* **184**, 383 (1969).

<sup>6</sup>P. Sigmund, A. Oliva, and G. Falcone, *Nucl. Instrum. Methods*

**194**, 541 (1982).

<sup>7</sup>G. K. Wehner and D. Rosenberg, *J. Appl. Phys.* **31**, 177 (1960).

<sup>8</sup>J. Bartella and H. Oechsner, *Surf. Sci.* **126**, 581 (1983).

<sup>9</sup>W. O. Hofer, in *Sputtering by Particle Bombardment III*, edited by R. Behrisch and K. Wittmaack (Springer, Berlin, 1992), p. 15.

<sup>10</sup>D. E. Harrison, *Crit. Rev. Solid State Mater. Sci.* **14**, S1 (1988).

<sup>11</sup>W. Eckstein, *Computer Simulation of Ion-Solid Interactions* (Springer, Berlin, 1991).

<sup>12</sup>U. Conrad and H. M. Urbassek, *Nucl. Instrum. Methods B* **48**, 399 (1990).

<sup>13</sup>H. Gnaser and H. Oechsner, *Nucl. Instrum. Methods B* **58**,

- 438 (1991).
- <sup>14</sup>H. Gnaser and H. Oechsner, *Surf. Sci.* **251/252**, 438 (1991).
- <sup>15</sup>R. Jede, H. Peters, G. Dünnebier, O. Ganschow, U. Kaiser, and K. Seifert, *J. Vac. Sci. Technol. A* **6**, 2271 (1988).
- <sup>16</sup>H. Oechsner, *Plasma Phys.* **16**, 835 (1974).
- <sup>17</sup>J. P. Biersack, S. Berg, and C. Nender, *Nucl. Instrum. Methods B* **59/60**, 21 (1991).
- <sup>18</sup>W. Möller and W. Eckstein, *Nucl. Instrum. Methods B* **2**, 814 (1984).
- <sup>19</sup>W. Möller, W. Eckstein, and J. P. Biersack, *Comput. Phys. Commun.* **51**, 355 (1988).
- <sup>20</sup>J. P. Biersack and L. G. Haggmark, *Nucl. Instrum. Methods* **174**, 257 (1980).
- <sup>21</sup>J. P. Biersack and W. Eckstein, *Appl. Phys. A* **34**, 73 (1984).
- <sup>22</sup>W. Eckstein and W. Möller, *Nucl. Instrum. Methods B* **7/8**, 727 (1985).
- <sup>23</sup>B. Baretzky, W. Möller, and E. Taglauer, *Nucl. Instrum. Methods B* **18**, 496 (1987).
- <sup>24</sup>W. D. Wilson, L. G. Haggmark, and J. P. Biersack, *Phys. Rev. B* **14**, 2458 (1977).
- <sup>25</sup>J. F. Ziegler, J. P. Biersack, and U. Littmark, *The Stopping and Range of Ions in Matter* (Pergamon, New York, 1985), Vol. 1.
- <sup>26</sup>K. A. Gschneidner, in *Solid State Physics*, edited by F. Seitz and D. Turnbull (Academic, New York, 1964), Vol. 16, p. 275.
- <sup>27</sup>H. Oechsner and W. Gerhard, *Surf. Sci.* **44**, 480 (1974).
- <sup>28</sup>W. Gerhard, *Z. Phys. B* **22**, 31 (1975).
- <sup>29</sup>G. P. Können, A. Tip, and A. D. de Vries, *Radiat. Eff.* **21**, 269 (1974).
- <sup>30</sup>H. Oechsner, in *Secondary Ion Mass Spectrometry SIMS III*, edited by A. Benninghoven *et al.* (Springer, Berlin, 1982), p. 106.
- <sup>31</sup>R. Kelly, *Surf. Interface Anal.* **7**, 1 (1985).
- <sup>32</sup>R. Kelly and A. Oliva, in *Erosion and Growth of Solids Stimulated by Atom and Ion Beams*, edited by G. Kiriakidis, G. Carter, and J. L. Whitton (Nijhoff, Dordrecht, 1986), p. 41.
- <sup>33</sup>M. W. Thompson, *Defects and Radiation Damage in Metals* (Cambridge University Press, Cambridge, 1969).
- <sup>34</sup>W. Eckstein and J. P. Biersack, *Appl. Phys. A* **37**, 95 (1985).
- <sup>35</sup>N. Andersen and P. Sigmund, *K. Dan Vidensk. Selsk. Mat. Fys. Medd.* **39**, No. 3 (1974).
- <sup>36</sup>P. Sigmund, in *Sputtering by Particle Bombardment I*, edited by R. Behrisch (Springer, Berlin, 1981), p. 9.
- <sup>37</sup>J. Bartella, Ph.D. thesis, Universität Kaiserslautern, 1985.
- <sup>38</sup>S. T. Nakagawa and Y. Yamamura, *Nucl. Instrum. Methods B* **33**, 780 (1988).
- <sup>39</sup>R. P. Webb and D. E. Harrison, *J. Appl. Phys.* **53**, 5243 (1982).
- <sup>40</sup>M. M. Jakas and D. E. Harrison, *Nucl. Instrum. Methods B* **14**, 535 (1986).